

# AuthGlass: Enhancing Voice Authentication on Smart Glasses via Air-Bone Acoustic Features

WEIYE XU, Tsinghua University, China

ZHANG JIANG, Tsinghua University, China

SIQI ZHENG, Tsinghua University, China

XIYUXING ZHANG, Tsinghua University, China

YANKAI ZHAO, Southern University of Science and Technology, China

CHANGHAO ZHANG, Ant Group, China

JIAN LIU\*, Ant Group, China

WEIQIANG WANG, Ant Group, China

YUNTAO WANG\*, Tsinghua University, China

With the rapid advancement of smart glasses, voice interaction has become widely deployed due to its naturalness and convenience. However, its practicality is often undermined by the vulnerability to spoofing attacks and interference from surrounding sounds, making seamless voice authentication crucial for smart glasses usage. To address this challenge, we propose AuthGlass, a voice authentication approach that leverages both air- and bone-conducted speech features to enhance accuracy and liveness detection. Aiming to gain comprehensive knowledge on speech-related acoustic and vibration features, we built a smart glasses prototype with redundant synchronized microphones: 14 air-conductive microphones and 2 bone-conductive units. In a study with 42 participants, we validated that combining sound-field and vibration features significantly improves authentication robustness and attack resistance. Furthermore, experiments demonstrated that AuthGlass maintains competitive accuracy even under various practical scenarios, highlighting its applicability and scalability for real-world deployment.

CCS Concepts: • **Do Not Use This Code** → **Generate the Correct Terms for Your Paper**; *Generate the Correct Terms for Your Paper*; *Generate the Correct Terms for Your Paper*; *Generate the Correct Terms for Your Paper*.

Additional Key Words and Phrases: Security, Voice Authentication, Bone-conduction, Sound Field

## ACM Reference Format:

Weiyue Xu, Zhang Jiang, Siqi Zheng, Xiyuxing Zhang, Yankai Zhao, Changhao Zhang, Jian Liu, Weiqiang Wang, and Yuntao Wang. 2018. AuthGlass: Enhancing Voice Authentication on Smart Glasses via Air-Bone Acoustic Features. In *Proceedings of Make sure to*

\*Co-corresponding authors.

---

Authors' Contact Information: Weiyue Xu, Tsinghua University, Beijing, China, xuwy24@mails.tsinghua.edu.cn; Zhang Jiang, Tsinghua University, Beijing, China, jiangzhang20030102@gmail.com; Siqi Zheng, Tsinghua University, Beijing, China, ymzqwq@gmail.com; Xiyuxing Zhang, Tsinghua University, Beijing, China, zxyx22@mails.tsinghua.edu.cn; Yankai Zhao, Southern University of Science and Technology, Shenzhen, China, 12432726@mail.sustech.edu.cn; Changhao Zhang, Ant Group, Hangzhou, China, eleven.zch@antgroup.com; Jian Liu, Ant Group, Hangzhou, China, rex.lj@antgroup.com; Weiqiang Wang, Ant Group, Hangzhou, China, weiqiang.wwq@antgroup.com; Yuntao Wang, Tsinghua University, Beijing, China, yuntaowang@tsinghua.edu.cn.

---

Permission to make digital or hard copies of all or part of this work for personal or classroom use is granted without fee provided that copies are not made or distributed for profit or commercial advantage and that copies bear this notice and the full citation on the first page. Copyrights for components of this work owned by others than the author(s) must be honored. Abstracting with credit is permitted. To copy otherwise, or republish, to post on servers or to redistribute to lists, requires prior specific permission and/or a fee. Request permissions from [permissions@acm.org](mailto:permissions@acm.org).

© 2018 Copyright held by the owner/author(s). Publication rights licensed to ACM.

Manuscript submitted to ACM

Manuscript submitted to ACM

enter the correct conference title from your rights confirmation email (Conference acronym 'XX). ACM, New York, NY, USA, 24 pages.  
<https://doi.org/XXXXXXX.XXXXXXX>

## 1 Introduction

Nowadays, smart glasses have been rapidly advancing, with commercial products such as Microsoft HoloLens[4] and Ray-Ban Meta Glasses[7] demonstrating their potential across diverse domains, including entertainment, healthcare, education, and industrial applications. As smart glasses are closely integrated with the user's head that allows unique interaction potential, researchers explored numerous application scenarios accessibility support for visually impaired users[40, 60] and context-aware services[53, 72].

Among various interaction modalities, voice commands have emerged as one of the most widely adopted approaches on smart glasses[7, 8]. Voice interaction is intuitive, hands-free, and well-suited to scenarios where users' hands are occupied, such as driving[18, 30] and cooking[16, 50]. However, as smart glasses are exposed to ambient voices, such interactions are susceptible to potential attacks, leading to severe security risks[57]. To migrate this issue, various authentication methods has be proposed, including password entry[34], iris recognition [39, 46] and gaze features[24]. Nevertheless, voice authentication remains the most natural complement to voice command interfaces[57], as it does not require additional interaction modalities and preserves the hands-free advantage[61].

Although voice authentication has been extensively studied [38, 70, 76, 80], achieving that on smart glasses remains challenging, as only limited work has examined acoustic features tailored to this unique form factor. In contrast, for other wearable platforms such as smartphones and earables [14, 22, 27, 42, 52, 80], researchers have investigated a wide range of methods to enable voice authentication[14, 32, 42, 45, 52, 80]. While these approaches have demonstrated competitive accuracy, their direct transfer to smart glasses is non-trivial due to the unique form factor and acoustic constraints of eyewear.

To address this, we present AuthGlass, an approach that leveraged vibration features and sound field features captured by smart glasses to enhance voice authentication. One of the key aspect of our system is to leverage time delay matrix and energy decrease matrix that captures the changes of sound field as the feature for authentication. To design the system, we firstly implemented a smart glasses with 14 air-conductive and 2 bone-conductive microphones to comprehensively explore these two factors. Through multiple experiments, we validated that both vibration features and sound field features were effective for authentication, and achieved even better performance of up to 0.03 equal error rate when combining them together.

To evaluate the usability of AuthGlass, we further conducted attack experiments to assess its resilience against different types of attacks. The results show that both feature sets can effectively resist attacks, with success rates below 0.05. To further demonstrate the practical applicability of AuthGlass, we performed multiple experiments incorporating various real-world restrictions. The results indicate that the AuthGlass system maintains robust performance even under these practical limitations.

Our key contribution include:

- We propose AuthGlass, an approach that leveraged vibration features and sound field features captured by smart glasses to enhance voice authentication. One of the key factor is that we leveraged time delay matrix and energy decrease matrix as sound field feature.
- By a 42-subjects experiments, we validated that using vibration features and sound field features could enhance the performance of authentication, reaching an EER of less than 0.03.

- Through evaluation on the attack robustness and usability, we further validate the performance of AuthGlass under practical limitations.
- We release an high-quality audio dataset of 96kHz of synchronized data among 42 subjects for future researches.

## 2 Related Works

In this section, we briefly reviewed previous works focusing on voice interface on smart glasses, authentication for smart glasses and liveness detection for voice authentication. We also pointed out current gap for voice authentication on smart glasses.

### 2.1 Voice Interface for Smart Glasses

As smart glasses were limited with size and shape, voice user interfaces (VUIs) have long been explored for interactions on smart glasses due to its' naturalness and convenience. Apart from vision-based and gaze based interaction, which rely on heavy and energy consuming sensors, voice interface only requires lightweight microphones for interaction[56], making it widely incorporated by commercial products like Ray-ban Meta[7], Xreal One Pro[10], Rokid Glasses[8], etc. More importantly, voice input is suitable for real-time communication and conversation-based AI functions. Ray-ban Meta utilized voice interface to control AI-powered services, while researchers also explored AI potentials on smart glasses via voice interface, especially for visual impaired people[25, 55, 60, 67]. Moreover, voice interface offers a 'touchless' interaction for users and do not interfere with users' gaze attention, it is especially suitable for emergency medical services[84] and industries [41].

As smart glasses increasingly integrate with users' personal information, securing their voice-based interfaces has become a critical challenge. However, with the rapid advancement of generative AI, voice interface was hindered by various attacking methods [21, 37, 77]. As smart glasses are often exposed to surrounding speech and ambient noise, they are vulnerable to forged commands injected by adversaries[17, 44], leading to potential severe privacy breaches. Prior works[43, 75] show that authentication schemes relying solely on acoustic features remain vulnerable to diverse threats, including replay[69, 77] and synthetic speech attacks[73, 85], thereby lacking robustness. Most previous works failed to explore usable acoustic features that could be applied to smart glasses. Thus, with this in mind, we aim to comprehensively explore the around-head acoustic features by glasses, hence promoting the design of voice authentication.

### 2.2 Authentication Methods on Smart Glasses

To address the security challenges of smart glasses, researchers have explored a wide range of authentication methods across different modalities. Broadly, existing approaches can be categorized into knowledge-based and biometric-based methods [19]. Knowledge-based authentication relies on what users know, with passwords being the most common example [17, 23, 24, 34, 74]. While such methods can provide a reasonable level of security, they often impose additional cognitive and interaction burdens on users [19]. In contrast, biometric authentication leverages users' inherent traits [15], which are difficult to replicate and require no conscious memorization. A variety of biometric-based techniques have been investigated, including iris recognition [39, 46], gaze movement patterns [33, 83], facial shape features [35, 44, 48], and skull characteristics [63, 64]. Among these, voice has attracted growing interest as a biometric modality [32, 57], since it can be seamlessly integrated into the voice user interfaces (VUIs) that are already central to the interaction paradigm of modern smart glasses.

However, achieving reliable voice authentication on smart glasses remains challenging, as few studies have comprehensively explored acoustic features specifically suited to this form factor. For other wearable platforms such as smartphones and earables [14, 22, 27, 42, 52, 80], researchers have investigated a wide range of acoustic representations, including time-domain features [80], frequency-domain features [32], time–frequency features [42, 45], and sound-field features [14, 52]. While these approaches have demonstrated high accuracy, their direct transfer to smart glasses is non-trivial due to the unique form factor and acoustic constraints of eyewear. In particular, smart glasses face challenges such as limited flexibility in microphone placement, variable distance from the user’s mouth, and increased susceptibility to ambient noise. All of these challenges hinder the straightforward adaptation of existing acoustic authentication techniques. Motivated by these challenges, we investigate features derived from both air- and bone-conducted acoustic domains, and evaluate their effectiveness in supporting robust voice authentication for smart glasses.

### 2.3 Liveness Detection for Voice Authentication

Beyond distinguishing users from impostors, voice authentication must verify that commands are genuinely produced by the user, a process referred to as liveness detection [12, 45, 47, 65, 79, 81]. To achieve this, researchers have proposed various methods, which can be categorized into speaker detection and speech detection. Speaker detection methods aim to determine whether a given sound originates from an artificial source, typically by exploiting features associated with machine-based speech production mechanisms, such as acoustic features [11, 47] and magnetic features [20]. However, these methods are tailored to the specific design characteristics of certain artificial speakers, which inherently limits their generalizability. As speech synthesis and voice conversion technologies continue to advance, such approaches may face increasing risks of being circumvented, thereby undermining their robustness in practical deployment.

Speech detection methods, in contrast, exploit features directly associated with the speaking process to ensure that the captured signal is temporally aligned with the user’s actual speech production [45, 62, 78, 82]. Building on this idea, researchers have explored a range of approaches, including throat vibrations [62], bone-conducted vibrations [45], facial muscle movements [82], airflow during articulation [71], and pop sounds [70], among others. While these studies have achieved promising results, most of them depend on sensors that either require close contact with the skin [32] or must be placed at locations impractical for everyday wearable devices (e.g., the throat) [62]. Such constraints not only affect user comfort and social acceptability but also hinder seamless integration into mainstream wearables, particularly smart glasses. To address these challenges and enable practical voice authentication on smart glasses, we further investigate the feasibility of leveraging combined acoustic features for liveness detection.

## 3 Understanding Air-Bone Acoustic Features by Smart Glasses

Previous studies have demonstrated the potential of speech-related acoustic features for authentication. However, their applicability to smart glasses remains unclear. In this section, we investigate acoustic features that potentially enhance voice authentication on smart glasses, with the goal of informing the design of more robust authentication systems.

### 3.1 Principle and Possibility

To understand how smart glasses can leverage voice-related features for authentication, it is essential to briefly review the human speech production system, as illustrated in Fig. 3a. Airflow from the lungs excites the vocal folds, the vocal tract then shapes this excitation into an acoustic realization with characteristic amplitudes and spectra [13]. After that, through precise control of the tongue and muscles, humans can articulate different phonemes and ultimately

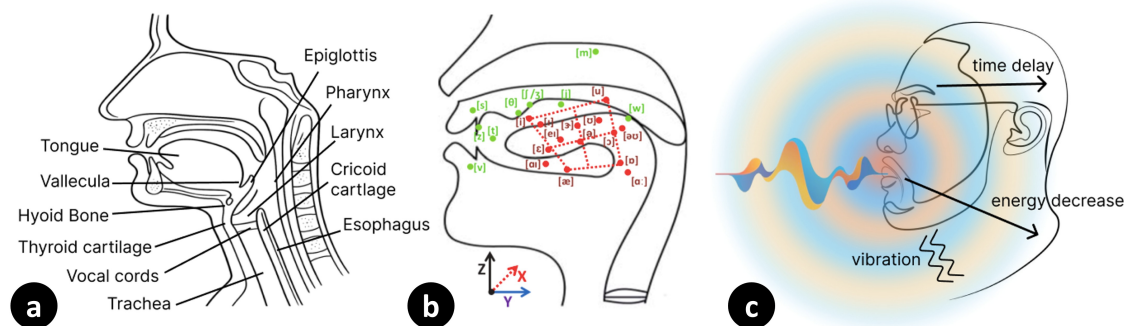


Fig. 1. (a) Structure of vocal tract, including vocal cords, tongue and other articulatory organs (b) Previous research revealed that phoneme sounds could be localized by method of Time Difference by Arrival [80]. (c) The possible acoustic features related to speech production, including vibration conducted by skin and bones, time delay and energy decrease of sound field in spatial dimension.

form words and sentences. Crucially, speaker-specific anatomy yields distinct propagation paths, resulting in both post-utterance signals and corresponding transmission paths carrying user-unique signatures for authentication.

However, existing approaches are based on features extracted from either the post-utterance voice or the transmission path, limiting comprehensive usage of the voice generation process. Most researchers focus on post-utterance features including airflow [71], pop-sound [70], and knowledge/content-based cues built from the observed speech signal. In contrast, motion-based methods that leverage IMU sensors in smart glasses exploit propagation-induced vibrations of the head/face but have limited access to the linguistic/ phonic content itself—and in smart glasses[82]. We therefore ask: how to integrate voice features with transmission-path cues on smart glasses to enable more robust authentication?

In this paper, we found smart glasses offer two potential sensing avenues that jointly encode voice features and how it propagates (Fig. 3b–c). First, air-conduction (air) microphone arrays in the frame enable capturing both the voice and the path-dependent spatial features of the surrounding sound field shaped by head geometry and motion of the articulator [80]. A bone/skin-conduction microphone (bone) at a stable contact point (e.g. nose pads) senses the voiceprint plus the propagation-induced vibrations transmitted through tissue and bone [49]. Thus, both channels inherently provide comprehensive features along the voice generation process, potentially enabling more robust authentication for smartglasses.

### 3.2 Capturing Air-bone Acoustic Features on Smart Glasses

**3.2.1 Design and Implementation.** As shown in Fig. 2a, we designed an eyeglass prototype based on real human head size. The frame measures 167.0 mm in length and 145.3 mm in width.

To capture the sound field as accurately and comprehensively as possible, we arranged a total of 14 omnidirectional air-conduction (AC) microphones around the user’s head (infineon IM73D122V01[3]) and oriented most of them downward. To maximize generality, our placement strategy spans multiple commercial form factors — including Ray-Ban Meta (nose bridge and legs), Bose Frames (behind the ears). We also integrated microphones on the rims as some prior work also investigated acoustic-based interaction and health sensing at the same locations [28, 29].

In order to capture vibration features, we employed bone-conduction microphones (VPU14AA01 BC)[9] for data collection, as they provide reliable sensing when in direct contact with the skin. Since smart glasses only make stable contact with the head around the nose and ears, and pilot studies showed that microphones near the ears were easily

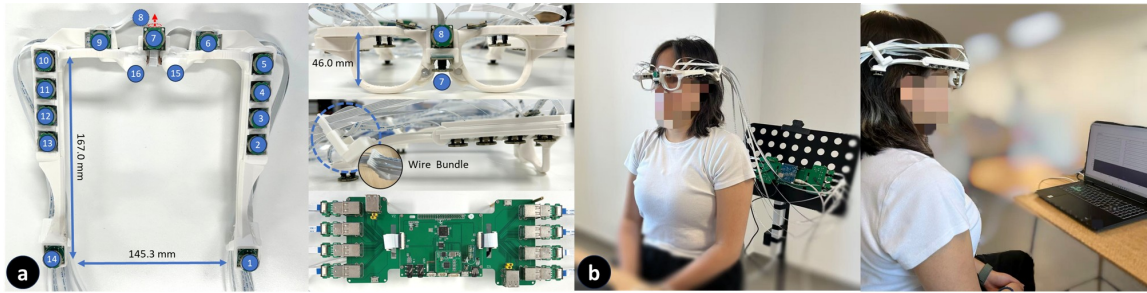


Fig. 2. a) Structural and hardware demonstration of the prototype. The prototype includes 14 channels of air-conductive microphones and 2 channels of b) Illustration of a user wearing the smart glasses prototype.

affected by hair friction, we mounted the bone-conduction microphones on each side of the nose pads to ensure better recording quality. The overall microphone layout is illustrated in Fig. 2a.

To acquire high-fidelity acoustic signals and extract meaningful insights, both bone-conduction and air-conduction microphones were configured in synchronization with a 96 kHz sampling rate. To achieve this, a collection board was used to connect all microphones simultaneously via flexible flat cables (FFCs), as shown in Fig.2a. The collection board was driven by an Orange Pi[6], which also transmitted data to a PC over a network cable using the TCP protocol. Note that a wire bundle was designed to prevent crosstalk between adjacent FFCs and to keep the cables organized, while maintaining user comfort.

**3.2.2 Data Collection.** We recruited 42 participants (14 female, 28 male), aged 18 to 42 (mean 24.6 +- 4.28), for data collection. To simulate different authentication scenarios, participants were required to repeat the listed short command sentences (see appendix) at three speaking volumes, each recorded twice. Soft volume was defined as speaking quietly, as if talking to oneself; medium voice resembled normal conversation with someone nearby; and loud voice approximated addressing someone 5 meters away. A total of  $42 * 6 * 15$  sentences were recorded through 16 synchronized microphones for analysis.

### 3.3 Key Findings and Insights

After data collection, we then analyzed the acoustic features of speech. Based on the mechanisms of human speech production, we examined features that capture the unique characteristics of individuals when speaking by vibration characteristics and sound field features.

**3.3.1 Acoustic Vibration Features.** Using the bone-conduction (BC) microphones embedded in the nose pads, we collected two channels of vibration signals. As some users maintained close contact with only one side of the nose pad, we selectively utilized the channel that yielded the more stable signal. Previous studies have demonstrated a correlation between signals captured by bone-conduction microphones and air-conduction microphones on earphones[45]. Motivated by this observation, we compared the BC microphone output with that of the channel 7 (Fig 2 a) AC microphone, as it was located most closely to user’s mouth and captured most detailed signal. Fig.3 demonstrate a comparison of Mel-spectrogram of AC and BC signals. In line with prior work, the Mel-spectrograms of these two kind of microphones exhibited relative consistency during speech, and both of them successfully aligned with phoneme boundaries processed by Munich Automatic Segmentation System (MAUS[5]). We also compared the outputs of BC and AC microphones

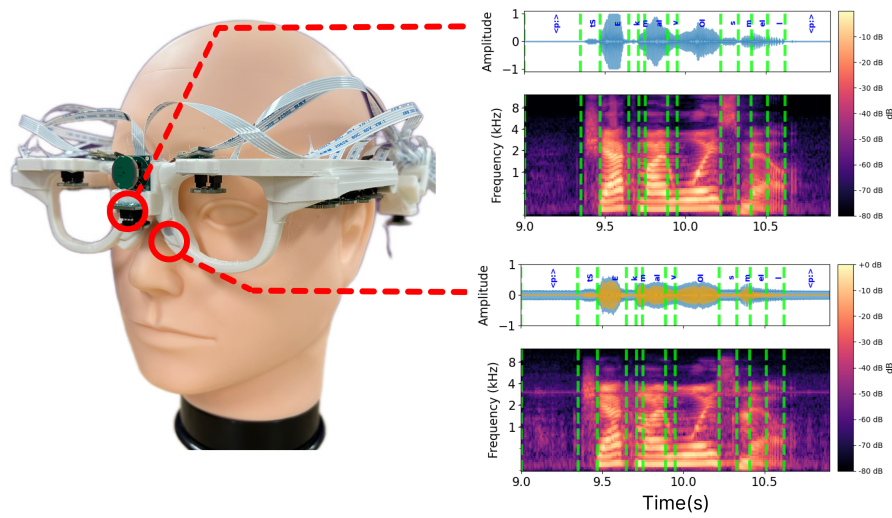


Fig. 3. Raw data from AC BC microphone and their Mel spectrum with phoneme segmentation by MAUS.

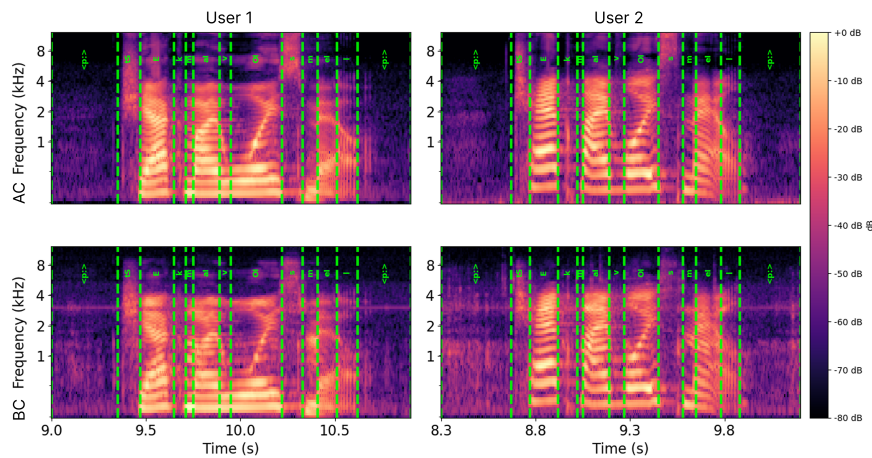


Fig. 4. Mel-spectrograms of acoustic signals collected from different users using AC and BC microphones.

when different users spoke the same sentence, as shown in Fig.4. While both BC and AC signals were able to capture speech, they exhibited noticeable differences above  $4\text{kHz}$ . Therefore, we regarded them as distinct and usable features.

**3.3.2 Sound Field Features.** As previous study revealed that the time delay [80] and energy difference [76] of a certain sound wave could act as distinctive features for authentication, we tried to explore the sound field feature through these two aspects. Fig. 5a demonstrates comparison of audio data on different AC channels during a certain fraction of time. Since the AC microphone located above the nose and oriented downward (channel 7 in Fig 2) received the strongest

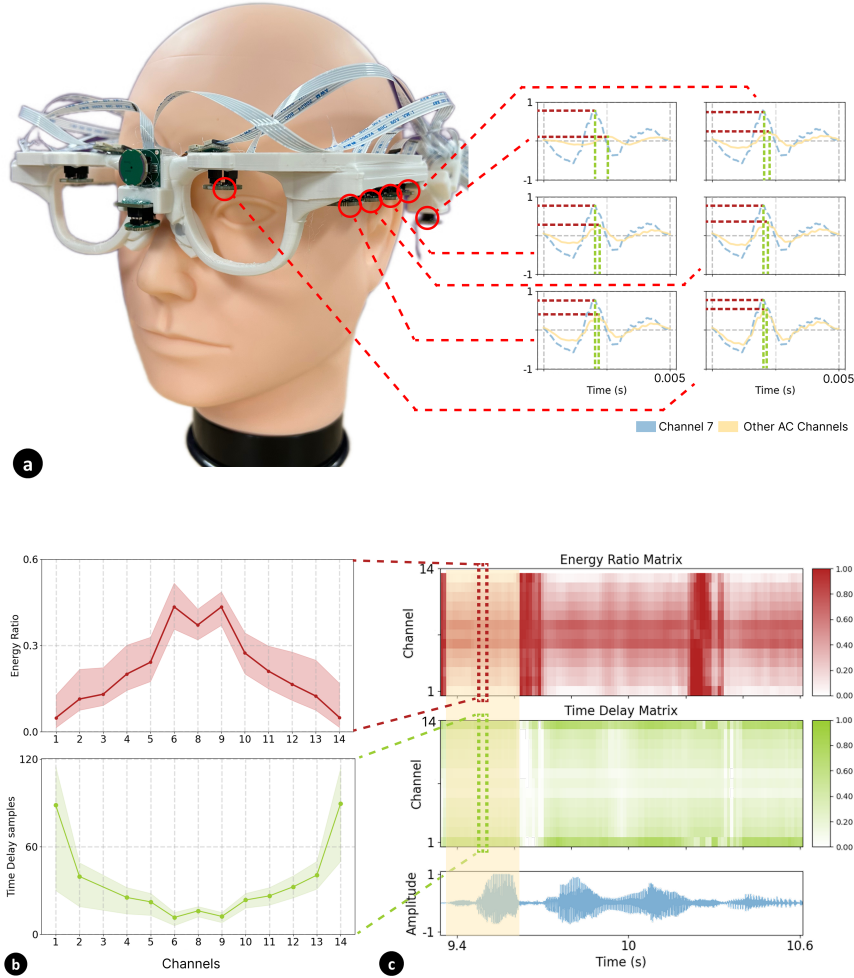


Fig. 5. (a) Waveform differences between the reference AC microphone (channel 7) and other AC microphones, with amplitude differences and time delays annotated across channels. (b) The average time delay and energy ratio (using channel 7 as reference). The shaded area indicates the variation range. (c) Energy delay matrix (EDM) and time delay matrix (TDM) for a speech segment.

energy, we utilized it as the reference channel and compare it with channels alongside one of the rim respectively. We observed that for channels along the rim, the relative audio energy with channel 7 decreased as the distance between the microphone and the mouth increased, while the time delay increased at the same time. Considering that the sound field may vary during people speaking, we detailed the changes by segmenting the audio into pieces, and calculated the energy ratio and time delay of all channels during each frame, forming an Energy Decrease Matrix (EDM) and a Time Delay Matrix (TDM), as shown in Fig 5c. From the figure, we noticed that the energy ratio and time delay captured by microphones at the position fluctuates continuously, which speaks to the facial movement of users.

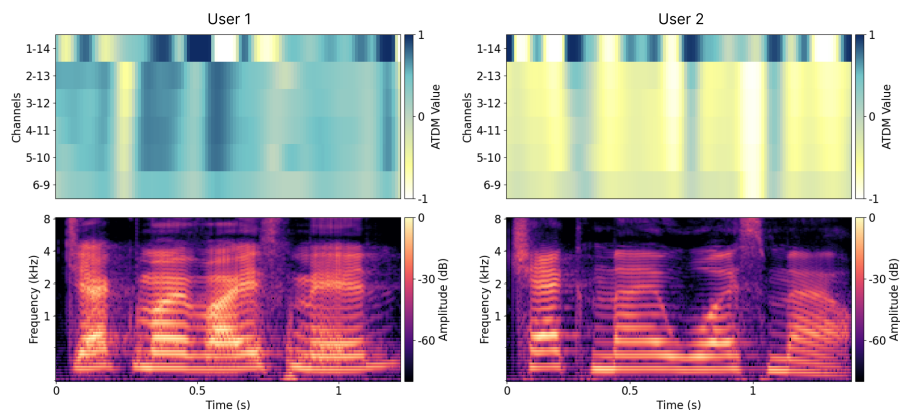


Fig. 6. TDM asymmetry and Mel-spectrograms of speech segments from different users. In the TDM asymmetry figure, blue indicates that the time delay on the right side when wearing the smart glasses is greater than that on the left, whereas yellow indicates the opposite.

Also, by measuring the changes of EDM and TDM alongside the time axis, we found that the maximum and minimum value of symmetrical pairs of AC microphones have noticeable difference, which speaks to the subtle asymmetry when capturing audios. To further evaluate this asymmetry, we calculated the time delay and energy ratio difference of symmetrical pairs by different users. Fig 6 demonstrated that different users produce subtle asymmetry patterns even when speaking the same content, making TDM and EDM potential features for authentication and anti-spoofing.

#### 4 Using Air-Bone Features for Liveness Authentication

Section 3.3 provides a thorough analysis of potential features for smart-glasses liveness authentication. However, their practical applicability and effectiveness remain unclear. We therefore instantiate a simple, representative authentication pipeline and empirically evaluate these features.

##### 4.1 Overview of the Authentication Structure

To begin, we define an authentication framework based on prior research[19, 32, 49]. Since our primary focus is on analyzing the acoustic features captured by smart glasses, we adopt a simple structure as the fundamental design. Fig. 7 illustrates our authentication model, which consists of three main modules: data pre-processing, liveness detection, and user authentication.

Upon using, user need to firstly conduct **enrollment**, passing his or her voice commands into the system for primary pre-processing. The pre-processing module then filters out noise and extracts usable features, and utilize a feature embedding algorithm to generate a template as key information for authentication. This template is saved for future authentication by the certain user via voice command.

During **authentication**, the user need to speak the certain authentication command. Then, the system pre-processes the received audio for feature extraction, following the same procedure as in enrollment. Unlike enrollment, however, the extracted features are passed to the liveness detection module, which determines whether the speech originates from the wearer of the smart glasses. Subsequently, the authentication module computes the embedding using the same algorithm as in enrollment and verifies the user by comparing the stored template with the incoming embedding.

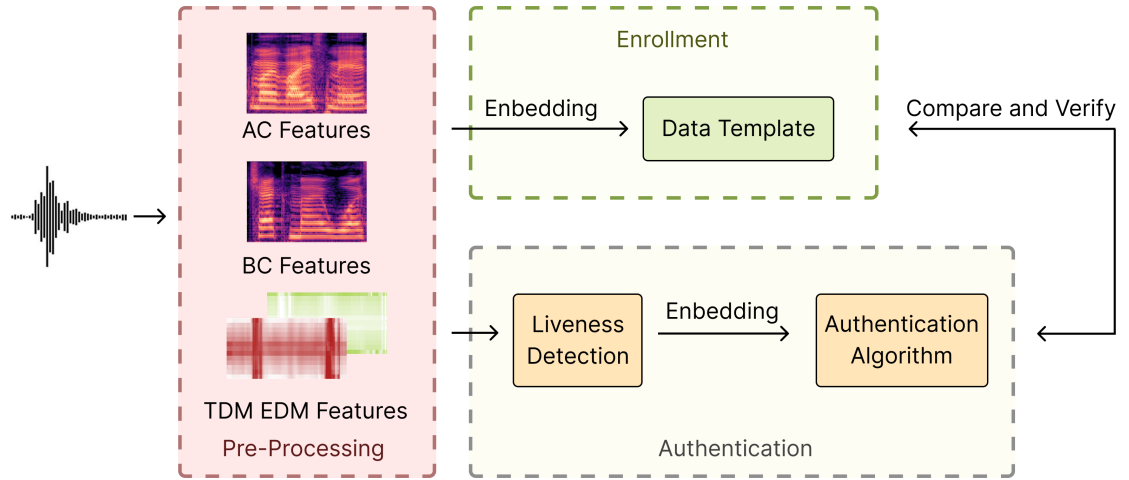


Fig. 7. Pre-processing exploits the features and utilizes a feature embedding algorithm to generate a data template. During authentication, features are passed to the liveness detection module and authentication algorithm compare the embedded data to the template.

## 4.2 Selected Features During Pre-processing

To evaluate the effectiveness of different features, we selected representative features for AC signal (voiceprint), vibration, and sound field, respectively. Firstly, we chose channel 7 (Fig 2a) AC microphone as baseline, since it captured most detailed air-conducted audio signal. To extract the voiceprint of this microphone, we incorporate common-used log Mel-spectrogram [51, 54] as the representative feature. Then, as demonstrated in section 3.3, vibration signals captured by BC microphones showed consistency with AC signals. Thus, we incorporate log Mel-spectrogram to process BC data, similar with AC feature. Finally, we opted TDM and EDM feature for sound field, as it speaks to the energy change and time delay variance during sound propagation.

## 4.3 Liveness Detection Through Vibration and Sound Field Features

Although prior studies have shown that a single AC microphone can be used for liveness detection[11, 47], their methods largely rely on artifacts specific to artificial speakers and may break down when facing different speaker types or adversarial strategies[59]. By contrast, leveraging speech-related biometric features offers greater robustness, as machines cannot fully replicate the human speech production process. Thus, based on findings from section 3.3, we utilized both the consistency between AC and BC signals, and a uniformed pattern of TDM and EDM across all users for liveness detection.

*4.3.1 Consistency between AC and BC signal.* To evaluate the consistency between AC and BC signal, we computed the correlation between the log Mel-spectrogram of these two signals at the same time. Fig. 8a shows the correlation scores across all sentences and users, where most cases exhibit high values, demonstrating a strong consistency of vibration and air-conducted acoustic signals when user is speaking. As Huang et al[32] proposed an alternative algorithm regarding the consistency, we leveraged this method for comparison with the algorithm parameters configured as  $M = 4$  and  $N =$

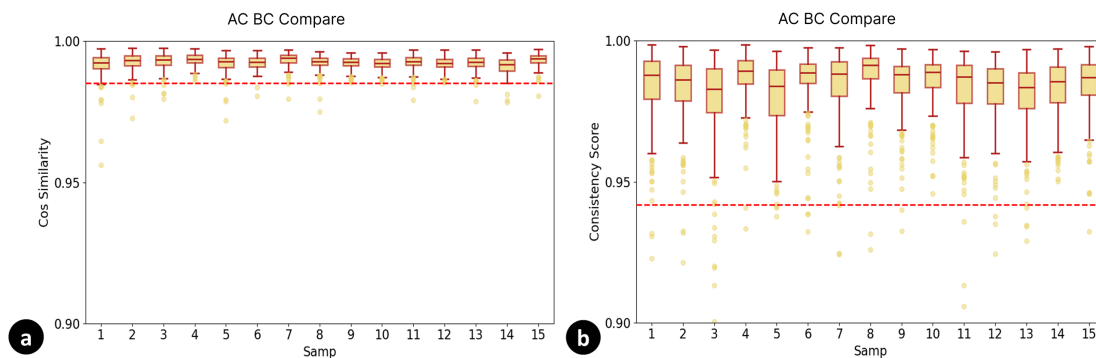


Fig. 8. Each box in the boxplot represents the interquartile range from the 0.25 to the 0.75 quantile, the red line indicates the median, the yellow dots denote outliers, and the red dashed line marks the 0.01 quantile. For (a) cosine similarity of Mel-spectrograms between AC and BC speech segments, the 0.01 quantile is 0.985, while for (b) the consistency score based on method from Huang et al[32] with parameter  $M = 4$ ,  $N = 4$ , the 0.01 quantile is 0.942.

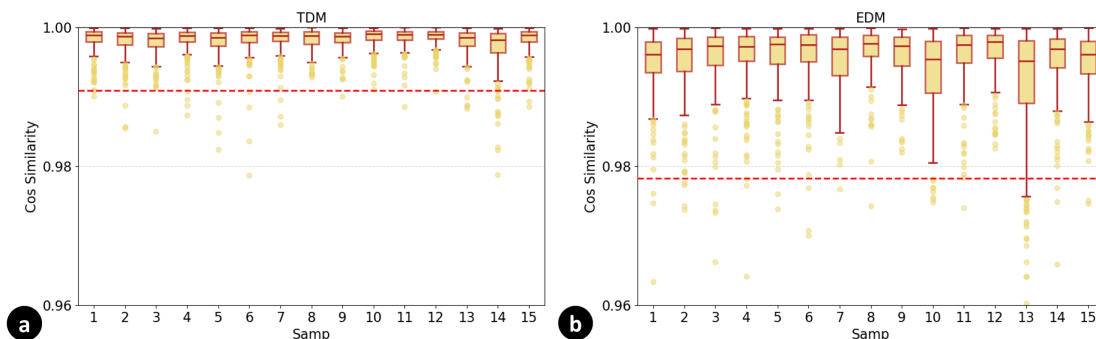


Fig. 9. Each box in the boxplot represents the interquartile range from the 0.25 to the 0.75 quantile, the red line indicates the median, the yellow dots denote outliers, and the red dashed line marks the 0.01 quantile. For (a) TDM cosine similarity between TDM and uniformed template, the 0.01 quantile for all sample is 0.991, while for (b) EDM cosine similarity, the 0.01 quantile is 0.978.

4, as shown in Fig 8. To balance the accuracy of the liveness detection system and its capability of rejecting adversarial samples, we set the acceptance rate at 99% and implemented the threshold for detection.

**4.3.2 Uniformed TDM and EDM pattern.** Since we have revealed the energy change and time delay variance along spatial dimension in section 3.3, we then tried to further incorporate it for liveness detection, as it speaks to where the received signal is from. To achieve this, we averaged the TDM and EDM along the time axis of each channels, forming a mean TDM and EDM template (similar with Fig 5b). Then we calculated the mean template across all users and all samples, resulting an uniformed TDM and EDM pattern. Finally, we calculated the cosine similarity between the uniformed pattern and template from all subjects, as shown in Fig 9. As all users exhibited high correlation value, we set the acceptance rate at 99% as the threshold with same consideration as section before.

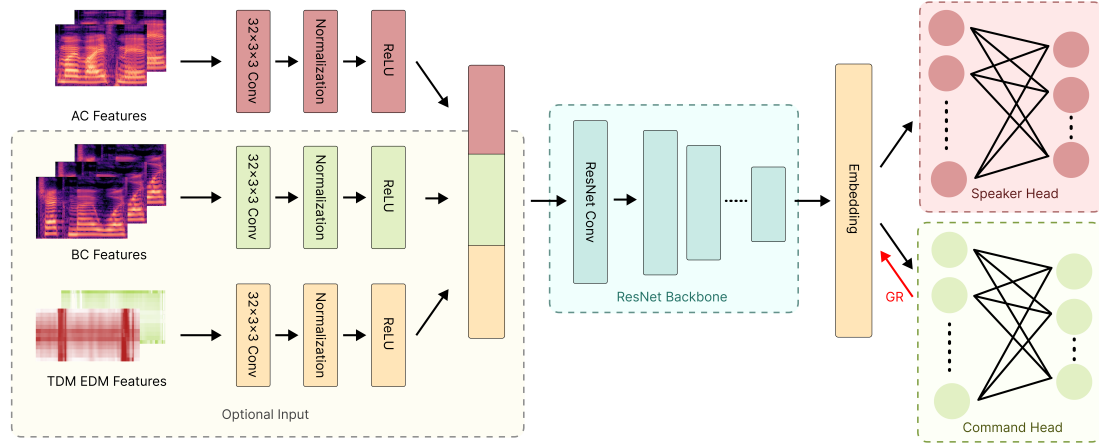


Fig. 10. The embedding model consists of four parts: head, ResNet backbone, command head and speaker head. The head allow 1-3 input features and we adjust the first layer of ResNet convolution to fit the input. Command head employs a gradient reversal layer to obfuscate command distinctions, making the model usable across all commands. Speaker head output the authentication result.

#### 4.4 Authentication by Various Features

**4.4.1 Principle for Embedding Algorithm.** After primary features were extracted, they were then embedded to a user-related feature either for enrollment or authentication, as described in section 4.1. Previous works have proposed different methods for embedding and comparison during authentication, such as Principal Component Analysis[36], Gaussian mixture model[49], and Deep Neural Networks[32]. As we aim to evaluate the effectiveness of various features, the embedding algorithm should be compatible with different input modalities. Furthermore, the algorithm needs to be independent of feature type, treating all modalities uniformly. Therefore, deep neural network (DNN) methods are the most suitable choice, owing to their flexibility and strong capability to extract embeddings for distinguishing different inputs.

**4.4.2 Embedding Algorithm Design.** During usage, users are required to authenticate using different voice commands, such as 'Pay the Bill' and 'Call Tom'. Therefore, it is necessary to employ a DNN model capable of accommodating various sentence inputs. Previous studies [32, 66] have shown that models based on ResNet [31] combined with domain-adversarial learning (DAL) [26, 68] achieve satisfactory accuracy with unsupervised domain adaption, which could be used for authentication across different commands. Based on this, as shown in Fig 10, we incorporated all convolution layers in ResNet18 as backbone structure and projected the output to a 256-dimension embedding by a fully connected layer. The embedding was then passed to two heads: the speaker head and the command head, representing the detected speaker and the command, respectively. To adapt to different combination of features, each input features processed by respective convolution head were concatenated together and then passed to the backbone model, where the input channel was expanded accordingly.

The training process of the embedding model served as a classification problem. During training, the model was fed with labeled data from the training set and optimized by minimizing the combined entropy loss from the speaker and command heads. The latter employs a gradient reversal layer to obfuscate command distinctions, thereby encouraging the DNN to learn embeddings that remain usable across all commands. After training, we discarded the speaker and

command heads and retained only the embedding layer to generate user embeddings for enrollment and authentication, assuming that the shared backbone captures representative information of individual characteristics regardless of the specific command.

*4.4.3 Enrollment and Authentication.* With a pre-trained embedding model, new users can enroll by speaking a designated voice command while wearing the glasses. Voice commands from different scenarios are recorded and mapped to multiple embedding vectors, which are then averaged to form a template vector for user authentication. During authentication, the user simply speaks the voice command, which is converted into an embedding vector. The system then computes the cosine similarity between this embedding and the stored template to verify the user.

## 4.5 Evaluation on Authentication Performance

*4.5.1 Method.* After designing the liveness authentication process, we aimed to investigate whether the selected features could support authentication and to assess their relative performance. To this end, we defined several feature groups, using the case that relies solely on the AC feature as the baseline, since it directly reflects the speaker’s voiceprint. We then assessed the contribution of vibration and sound field features when combined with AC signals, denoted as AC + BC and AC + DMs (where DMs refer to TDM + EDM), respectively. Finally, we evaluated the performance using all three types of features—AC, vibration, and sound field—denoted as AC + BC + DMs. In addition, as a training baseline, we used the straightforward sound field feature—the log Mel-spectrograms from all channels except the reference AC channel—denoted as SF, and conducted experiments similar to those with DMs.

For each feature group, we performed a 7-fold cross-user evaluation on the data collected from 42 subjects. In each fold, the data of 36 subjects were used for training with a 10-times data augmentation on the audio amplitude, while the remaining 6 subjects were reserved for testing authentication accuracy. For enrollment, each test user provided one sample per command to simulate real-world usage, and the system averaged the corresponding embeddings to construct that user’s template. Then, we evaluated the performance of authentication using Equal Error Rate (EER) [32] as metric, as it gives a balanced measurement on both the false acceptance and false reject. Given the limited dataset size and our focus on exploring the potential of different features, no validation set was employed. Each training trial ran for 50 epochs, and the authentication EER was evaluated every 5 epochs. Model that reached lowest EER during 50 epochs were selected and the EER metrics as long as the threshold for cosine-similarity calculation were averaged across 7 folds.

	AC	AC+DMs	AC+SF	AC+BC	AC+BC+DMs	AC+BC+SF
mean EER	0.09	0.05	0.08	0.05	0.03	0.06
mean threshold	0.49	0.61	0.53	0.58	0.62	0.66

Table 1. Averaged EER and threshold of Different Feature Combination.

*4.5.2 Result and Discussion.* Table 1 shows the averaged EER and threshold of different feature combination across 7 folds of experiments. As illustrated, AC + BC and AC + DMs combination yields approximate 0.05 decrease on EER compared with single AC group, indicating that both vibration signal (BC) and sound field features could be leveraged to enhance authentication performance respectively. Furthermore, combining the BC and DMs feature could achieve better result with even lower EER. In contrast, using SF features as an end-to-end methods proved to be not that effective, as

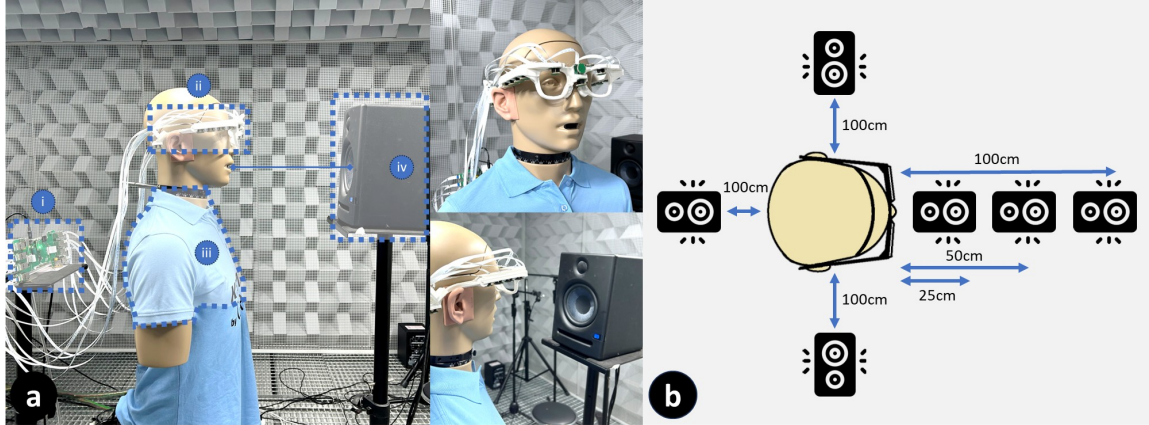


Fig. 11. (a) The environment setting of the voice attack. i and ii are smart glasses prototype, iii is the torso-mouth simulator and iv is the loudspeaker. In the experiment, two types of attack were applied: loudspeaker replay attacks and a torso-mouth simulator attacks which replicates the exhalation process and torso vibrations during speaking. (b) In the replay attack, the loudspeaker was placed at different positions and distances from the smart glasses to simulate various attack situations.

AC + SF group only has a slight EER decrease compared with single AC ones and there is no difference between AC + BC + SF group and the AC + BC ones. Thus, we leverage DMs as the sound field feature as it can capture both energy changes and time delay variance.

## 5 Robustness Against Attack

After the primary evaluation on the authentication system, we then tested its' effectiveness against attack, as this speaks to whether the system could be applied to real-world usage.

### 5.1 Attack Model

Similar with section 4, we need to firstly define the attack model. With the rapid advancement of audio generative methods[37, 73], solely rely on audio features to defend against certain kinds of adversarial sample could not guarantee the effectiveness of the authentication system. Therefore, we designed the attack evaluation based on two assumptions. (a) the attacker can perfectly capture and replay the air-conductive signals and (b) the attacker could be able to simulate the speech production process, but cannot perfectly replicate that of each individuals. A total of three attack experiments were conducted.

### 5.2 Experiment 1: Attack by Simulated Wearer

**5.2.1 Method.** Considering when an attacker could access the smart glasses device, we aimed to use an simulator to attack the authentication system. Thus, as shown in Fig 11a, we incorporated GRAS-45BC-KEMAR[2], a torso-mouth simulator to generate adversarial samples. The simulator could not only produce high-quality audio but could also simulate the exhaling process and torso vibration during speaking, making it a perfect example to generate audio samples as well as the vibration and sound field features.

To collect the attack samples, we placed our smart glasses prototype onto the simulator's head, mimicking the scenario during usage. Then, we utilized the genuine signal from channel 7 AC microphone, played these audio through

the simulator, and collected the data through our smart glasses prototype. All samples collected in section 3.2.2 were used to generate adversarial data. Note that we balanced the volume for the attack samples before and after the collection, aiming to fully mimicking the original audios.

Then, with these adversarial samples, we attack the models trained in section 4.5 separately following the 7-fold group. For each groups of data, we followed the enrollment process same as those in 4.5 via one original sample per command, and then attack using the collected attack samples divided into folds respectively. To evaluate the effectiveness of the methods for liveness detection in section 4.3 we calculated the pass rate (PR) of the attack samples by these methods. For simplicity, we denoted the consistency between AC and BC signals calculated by cosine similarity as **CS1**, while the method from Huang et al[32] as **CS2**. For the method using uniformed TDM and EDM pattern, we just denoted them as TDM and EDM respectively. Though there was only partial of attack samples passed through liveness detection, we still fed all attack samples to the authentication system for comprehensive evaluation. We utilized Attack Success Rate (ASR) to evaluate the system’s robustness against attack.

	CS1	CS2	TDM	EDM
PR	0.004	0.998	0	0.998

(a) PR for four liveness detection metrics

	AC	AC+BC	AC+DMs	AC+BC+DMs
ASR	0.1596	0.0077	0.0491	0.0003

(b) ASR for different feature combinations

Table 2. Averaged Passing Rate (PR) and Attack Success Rate (ASR) for experiment 1.

**5.2.2 Result and Discussion.** Table 2 demonstrated the PR for four types of liveness methods and the ASR for four types of feature combination, following the configurations in section 4.5. Since SF feature did not yield significant promotion on authentication performance, we did not incorporated this feature for ASR calculation. As shown in the table, CS1 yields lower pass rate, meaning that it’s suitable for smart glass scenario compared with CS2, which only gives rough estimation on the consistency of AC and BC signals.

As shown in table 2b, both BC signals and sound field feature (DM) promote the resilience against attack, while combining them together reached the lowest ASR rate. This indicating that vibration signals and sound field features could both be contributive for authentication.

### 5.3 Experiment 2: Attack by Nearby Sound Source

**5.3.1 Method.** Apart from direct attack by simulated wearer, voice authentication on smart glasses could suffer from attack from sound source from environment, as the devices are exposed to surrounding voices. Therefore, we utilized PreSonus Eris E5[1], a high-quality speaker as the attacker sound source. To control the relative position between user and attacker, we leveraged the simulator used in previous experiment as the user with fixed position when putting the smart glasses on. Then, we selected six position located on four direction of the simulated user, as shown in Fig 11b. Similar with experiment 1, we utilized all the genuine samples for attack and balanced the volume for different attacking points. After getting the result following the 7-fold division. Since all the PR achieved to 0, we only averaged the ASR of all attacking position for evaluation.

**5.3.2 Result and Discussion.** Table 3 demonstrated the PR for four types of liveness detection and ASR for four types of feature combination, following the configurations in section 4.5. For liveness detection, both the AC-BC consistency reached a relatively low performance with 0.65 passing rate, we concluded that the bone-conductive microphone were

	AC	AC+BC	AC+DMs	AC+BC+DMs
ASR	0.0960	0.0310	0.0338	0.0204

Table 3. Attack Success Rate (ASR) for experiment 2.

affected by the air-conducted signal. Since the audio collection room incorporated noise canceling configurations, the AC channel could be consistent with the BC signal. For TDM and EDM template, TDM yielded best performance as the signal is not from the mouth, leading to a total different TDM pattern. While for EDM, it cannot capture Similar with previous experiment, combining DM and BC yielded the best performance.

### 5.4 Experiment 3: Synthetic Attack Using Original Audios

*5.4.1 Method.* Although we incorporated high quality method to generate attack samples and tested the defending capability of the proposed authentication system in experiment 1 and 2, there’s still a chance that the adversarial samples did not accurately reconstruct the original audio features. Thus, we substituted the AC features in all attack samples of previous experiments with the genuine ones, and utilized these synthesized features as attack samples and re-evaluate the performance of the authentication system. By conducting the evaluation, we could gain further understanding of whether vibration signals and sound-field features could enhance the authentication performance, as the adversarial samples share the same AC features with the genuine data. Since the evaluations on liveness detection were conducted before, we only considered the ASR of different combination of features, and neglected the AC group since we leveraged the actual AC feature for authentication.

	AC+BC	AC+DMs	AC+BC+DMs
Simulated Wearer	0.0046	0.1046	0.0167
Nearby Sound Source	0.0306	0.0408	0.0027

Table 4. Averaged Attack Success Rate (ASR) for experiment 3.

*5.4.2 Result and Discussion.* Table 4 demonstrated the ASR for three types of feature combination. As shown in the table, incorporating genuine AC features substantially increases the ASR for AC+DMs in the simulated-wearer case, indicating that DM features alone are not sufficiently discriminative to block attacks when the simulated wearer closely resembles the genuine user. In contrast, for the nearby sound source scenario, both DMs and BC demonstrate a relative ability to resist attacks originating from surrounding voices.

## 6 Usability of AuthGlass

Since the evaluation of the authentication system remained at a prototype stage, the practicality of the proposed method was still uncertain. Therefore, in this section, we assess the performance of the AuthGlass system under various real-world conditions to better demonstrate its applicability.

### 6.1 Restricted Microphone Number

Aiming to exploit a throughout acoustic features by smart glasses, we embedded 14 AC microphones and 2 BC ones, which were redundant compared with commercial smart glasses. Realizing this, we investigated whether leveraging a

limited number of microphones could achieve a competitive authentication performance. Based on various designs of modern smart glasses, we selected two representative cases: a 3-channel microphone array such as Rokid[8] and a 5-channel microphone array such as Rayban Meta[7]. To evaluate the performance of these two kinds of configurations, we selected the specific AC microphone combination on our prototype to simulate the microphone layout, as shown in Fig 12. In these cases, the microphone number was restricted and sound field feature could only be partially captured. Despite this, considering the effectiveness of EDM and TDM feature in representing sound field, we still leveraged the corresponding channels of AC microphone to compute these two features. Then, we retraced the evaluation steps in section 4.5, including embedding model training, enrollment and authentication process. Then, we calculated the EER among 7-folds of data to evaluate the performance under limited microphone settings. As shown in Fig 12. Result shows that as the channel number increased, the performance using sound field features increase accordingly, while BC signals have better performance compared with sound field features. Also, three channel sound features did not yielded better performance due to the insufficient sound field information.

## 6.2 Cross-Session Validation

**6.2.1 Method.** In practical applications on smart glasses, authentication systems are expected to deliver stable results across different wearing sessions. Unlike controlled laboratory settings, users may wear the device at varying times or under slightly different conditions. Thus, to ensure reliability, the system must exhibit cross-session robustness, meaning that the authentication outcome remains consistent every time the device is worn. To validate the cross-session performance, we recruited 23 of the 42 subjects in section 3.2.2 again, and asked them to redo the same process as that during data-collection. Then, using the model that has already trained, we conducted the evaluation steps similar in section 4.5, leveraging the old data for enrollment (1 sample per command) while using the newly collected data to authenticate.

**6.2.2 Result and Discussion.** Table 5 demonstrated the Averaged EER of Different Feature Combination for Cross-Session Validation. The results demonstrate the averaged EER for different feature combinations in the cross-session validation. As shown in the table, all four feature sets achieve relatively high accuracy. Compared with the original EER obtained in the initial session, there is virtually no performance degradation, indicating that the authentication model maintains strong cross-session robustness and can consistently deliver reliable results across different wearing instances.

	AC	AC+DMs	AC+BC	AC+BC+DMs
mean EER	0.0981	0.0449	0.0861	0.0505

Table 5. Averaged EER of Different Feature Combination for Cross-Session Validation.

## 6.3 Robustness Against Noise

**6.3.1 Method.** For deployment on smart glasses, authentication systems inevitably face various sources of noise. Thus, to evaluate the robustness under noisy conditions, we introduced environmental noise into the input signals. Since our prototype captures data from synchronized multiple-channel AC microphones placed at certain layout, it is not appropriate to incorporate noises dataset from mono microphone. Therefore, we collected real-world ambient sounds from three typical scenarios: cafés, restaurants, and shopping malls using our smartglasses prototype, while

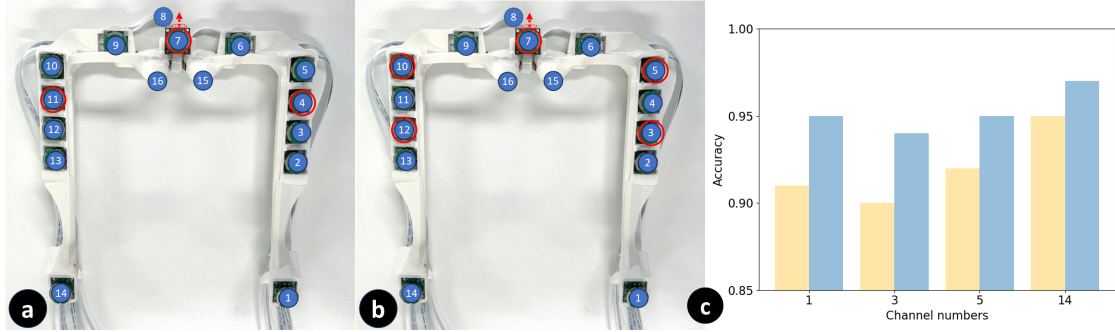


Fig. 12. In the restricted microphone experiment, TDM and EDM were calculated using three and five microphones, respectively. (a) shows the three microphones selected. (b) shows the five microphones selected. (c) presents the authentication accuracy using different number of microphones. Yellow indicates inputs containing only AC microphones, while blue indicates inputs containing both AC and BC microphones.

simultaneously recording the sound levels with a decibel meter. After collecting the noises, we mixed the noise with origin signals at certain degrees of signal-to-noise ratio (SNR), using channel 7 microphone as reference. With the data mixed with noises, we further tested the authentication performance by EER metric using the same model as 4.5 following the 7-fold settings.

**6.3.2 Result and Discussion.** As shown in Table 6, when the SNR decreases, the performance of all methods is degraded to a very high EER. Instead, for 10 SNR group, combining BC signals or sound field features did not enhance the performance, as the sound field features and BC audios could be affected when there are noises. Finally, for 20 SNR group, combining all the features yielded better performance than other groups, indicating that the system could be affected by high noises.

SNR (dB)	AC	AC+DMs	AC+BC	AC+BC+DMs
5	0.1491	0.1843	0.1593	0.1781
10	0.1046	0.1528	0.1417	0.1546
20	0.0898	0.0747	0.0849	0.0481

Table 6. Averaged EER of Different Feature Combination for Noisy Environment under Different SNR Levels.

## 6.4 Limited Sampling Rate

**6.4.1 Method.** Another aspect that limit the real-world usage was the sampling rate, as our prototype samples audio at a frequency of 96 kHz, requiring relatively high energy and memory demands. In contrast, most commercial smart glasses adopt microphones with a 16 kHz sampling rate. While such a rate has little effect on Mel-spectrogram computation, it can impact sound field modeling and time-delay estimation accuracy. To verify the effect of limited sampling rates on voice authentication, we down-sampled the acoustic data to 16 kHz, and re-tested the authentication EER, with other configurations same as those in section 4.5.

6.4.2 *Result and Discussion.* As shown in Table 7, our model continues to achieve strong performance at a lower sampling rate of 16kHz. The results indicate that our model performs well across different sampling rates, demonstrating robustness to variations in input resolution.

	AC	AC+DMs	AC+BC	AC+BC+DMs
mean EER	0.0917	0.0460	0.0648	0.0302

Table 7. Averaged EER of Different Feature Combination for 16kHz Sampling Rate.

## 7 Discussion

In this section, we first summarize the key findings of this work and then highlight the potential applications of the proposed system. Finally, we discuss its limitations and outline possible directions for future research.

### 7.1 Conclusion of Findings

Using our prototype, we observed that both vibration and sound-field features are closely related to human speech production. To extract these features, we applied the well-established log Mel-spectrogram method for vibration signals, and we further proposed two novel representations—time delay matrix (TDM) and energy decrease matrix (EDM)—to capture temporal variations in sound-field features. With a relatively simple authentication architecture, we demonstrated that vibration and sound-field features each improve authentication performance, and their combination yields even better results. Moreover, extensive experiments showed that the proposed AuthGlass system can effectively resist attacks while maintaining robust performance under practical conditions.

### 7.2 Potential Applications

As our proposed method operates as a fully passive voice authentication approach on smart glasses, it has the potential to be seamlessly integrated into modern wearable devices, enabling a wide range of applications. For example, because smart glasses are convenient to use while users are engaged in other activities with their hands occupied, such as driving and cooking[18, 30, 41], AuthGlass could enable hands-free authentication for tasks like signing an urgent document or opening the smart lock, minimizing distraction and allowing users to complete the task safely. Moreover, since smart glasses with voice user interfaces are particularly beneficial for visually impaired users [40, 60], our system can provide a secure authentication process without the risk of information leakage associated with traditional methods such as password entry. Last but not least, since voice authentication on smart glasses is closely linked to human attention, our system can be integrated with other sensors such as cameras, to enable natural interactions. For example, a user could simply look at a payment QR code and say “Pay the bill” to complete a transaction seamlessly

### 7.3 Limitation and Future Works

7.3.1 *More Configurations of AC Microphones.* Our study demonstrates the effectiveness of incorporating sound field features into voice authentication. However, we only tested limited choice of AC microphone combinations and did not optimal the combination and layout of the microphones, which could be vital for the design of microphones on smart glasses. To pave a way for future works, we will release our dataset to enable more researchers to explore different

microphone configurations, which would possibly be beneficial for better design of voice authentication system on smart glasses.

*7.3.2 Cross-device Adaption.* Though we demonstrated that vibration features and sound field features have a strong performance in liveness detection and authentication, they may face challenges in cross-device scenarios. For instance, different spatial layout of microphones will lead to different sound field signals, while the contact circumstance between vibration microphones and user skin may vary between devices, causing the vibration signal inconsistent. One of the possible solutions is to leverage cross-device adaption methods by modeling the sound field across humans, which could transit the data from one type of glasses to another. What's more, deep learning methods can be employed to enhance the generalization capability of the algorithms, as researchers have proposed unsupervised cross-domain adaptive methods [26].

*7.3.3 Robustness against Movement Noises.* Although we evaluated the performance of our system under noisy conditions, our experiments only considered scenarios in which users remained still. To support a wider range of applications, the authentication system should also be robust to noise generated by user movements. Specifically, head movements may affect vibration signals, as BC microphones can be sensitive to motion, similar to an IMU. Additionally, changes in head posture can influence the sound field features. To migrate this issue, one possible idea is to leverage additional motion-related sensors, such as IMU or gyroscope for denoising as prior works [75] has demonstrated the possibility of denoising on other motion-sensitive sensors, for example, the PPG sensor.

*7.3.4 Deployment to commercial devices.* As one of the key focuses of this work is the practical applicability of AuthGlass, several challenges remain for deployment on commercial devices. Although the TDM and EDM features proposed in this paper have been validated as effective, their computation still incurs a non-negligible processing time, which limits the feasibility of real-time authentication. In addition, the system relies on precise synchronization of the microphone arrays to accurately capture sound-field data, posing additional design and implementation challenges. Furthermore, there is currently no mature solution for embedding bone-conduction microphones into the nose pad of smart glasses, which may restrict both signal quality and overall system performance. Despite these limitations, advances in hardware and embedded systems present opportunities to overcome these challenges. Improved sensor integration, more efficient signal processing algorithms, and faster computation could not only resolve current hardware constraints but also enhance the real-time capability and robustness of AuthGlass, paving the way for its adoption in practical, commercial applications.

*7.3.5 Sound Field Based Interaction on Smart Glasses.* Our work demonstrates that sound-field features are related to the human speech production process, suggesting potential for broader applications. For example, Proximic [58] leveraged the time differences between a pair of earbuds to detect mouth-cover gestures. Building on this idea, sound field features could enable hands-on-mouth gesture detection during speech without relying on active acoustic sensing techniques [28]. Moreover, since the speech generation process can be influenced by the direction a user is facing, sound field features may also be used to infer the direction of the user's speech, thereby facilitating more natural and context-aware interactions.

## 8 Conclusion

This work addresses the challenges of voice authentication on smart glasses, particularly the limitations of methods that rely solely on voiceprints. By jointly leveraging vibration and sound-field features, our proposed system, AuthGlass,

achieves not only competitive authentication performance but also strong resilience against potential attacks. One key aspect of this system is to leverage time delay matrix and energy decrease matrix to represent sound field features. To validate the effectiveness of the system, we conducted a series of experiments that examined the contribution of individual features as well as their combination. Furthermore, we evaluated the system under various practical conditions, including limited microphone configurations, cross-session scenarios, noisy environments, and reduced sampling rates. The results consistently demonstrate the applicability and robustness of AuthGlass in real-world settings. Looking ahead, with advancements in hardware design and embedded processing, the system holds promise for seamless integration into commercial smart glasses, paving the way for secure and effective voice authentication in everyday scenarios.

## References

- [1] 2025. Eris® E5 Studio Monitor. [https://intl.presonus.com/products/eris-e5-studio-monitor?srsltid=AfmBOopFGpJKhO6xHwJ\\_iRWISQZsIO9KiW8Wv5WjZ0mKTitWmFcpOnO](https://intl.presonus.com/products/eris-e5-studio-monitor?srsltid=AfmBOopFGpJKhO6xHwJ_iRWISQZsIO9KiW8Wv5WjZ0mKTitWmFcpOnO).
- [2] 2025. GRAS 45BC KEMAR Head and Torso with Mouth Simulato. <https://www.grasacoustics.com/products/head-torso-simulators-kemar/kemar-non-configured/product/749-45bc>.
- [3] 2025. Infineon IM73D122V01: Ultra-low noise high sensitivity digital XENSIVTM MEMS microphone. <https://www.infineon.com/assets/row/public/documents/24/49/infineon-im73d122-datasheet-en.pdf?fileId=8ac78c8c83cd3081018409cafd646db>.
- [4] 2025. Microsoft Hololens. <https://learn.microsoft.com/en-us/hololens/>.
- [5] 2025. The Munich Automatic Segmentation System MAUS. <https://www.bas.uni-muenchen.de/Bas/BasMAUS.html>.
- [6] 2025. Orange Pi Zero2 Module. <http://www.orangepi.org>.
- [7] 2025. Ray-ban Meta. <https://www.ray-ban.com/usa/ray-ban-meta-ai-glasses>.
- [8] 2025. Rokid Glasses. <https://glasses.rokid.com>.
- [9] 2025. Sonion Voice Picking Unit VPU14aa01. [https://www.ariat-tech.com/parts/VPU14AA01?srsltid=AfmBOoqPZF0ySufKmsHCBWudGqWET3zyMni78FVCvMtjz08pOYW5\\_n](https://www.ariat-tech.com/parts/VPU14AA01?srsltid=AfmBOoqPZF0ySufKmsHCBWudGqWET3zyMni78FVCvMtjz08pOYW5_n).
- [10] 2025. Xreal One Pro. <https://www.xreal.com/one-pro>.
- [11] Muhammad Ejaz Ahmed, Il-Youp Kwak, Jun Ho Huh, Iljoo Kim, Taekkyung Oh, and Hyoungshick Kim. 2020. Void: A fast and light voice liveness detection system. In *29th USENIX Security Symposium (USENIX Security 20)*. 2685–2702.
- [12] Zahid Akhtar, Christian Michelon, and Gian Luca Foresti. 2014. Liveness detection for biometric authentication in mobile applications. In *2014 International Carnahan Conference on Security Technology (ICCST)*. IEEE, 1–6.
- [13] Pierre Badin and Antoine Serrurier. 2006. Three-dimensional modeling of speech organs: Articulatory data and models. In *Technical Committee of Psychological and Physiological Acoustics*, Vol. 36. The Acoustical Society of Japan, 421–426.
- [14] Logan Blue, Hadi Abdullah, Luis Vargas, and Patrick Traynor. 2018. 2ma: Verifying voice commands via two microphone authentication. In *Proceedings of the 2018 on Asia Conference on Computer and Communications Security*. 89–100.
- [15] Duttiff Boshoff and Gerhard P Hancke. 2025. A classifications framework for continuous biometric authentication (2018–2024). *Computers & Security* 150 (2025), 104285.
- [16] Bruno Bouchard, Kevin Bouchard, and Abdenour Bouzouane. 2020. A smart cooking device for assisting cognitively impaired users. *Journal of reliable intelligent environments* 6, 2 (2020), 107–125.
- [17] Pan Chan, Tzipora Halevi, and Nasir Memon. 2015. Glass otp: Secure and convenient user authentication on google glass. In *International Conference on Financial Cryptography and Data Security*. Springer, 298–308.
- [18] Wan-Jung Chang, Liang-Bi Chen, and Yu-Zung Chiou. 2018. Design and implementation of a drowsiness-fatigue-detection system based on wearable smart glasses to increase road safety. *IEEE Transactions on Consumer Electronics* 64, 4 (2018), 461–469.
- [19] Yun-Tai Chang. 2018. *A two-layer authentication using voiceprint for voice assistants*. Ph. D. Dissertation.
- [20] Si Chen, Kui Ren, Sixu Piao, Cong Wang, Qian Wang, Jian Weng, Lu Su, and Aziz Mohaisen. 2017. You can hear but you cannot steal: Defending against voice impersonation attacks on smartphones. In *2017 IEEE 37th international conference on distributed computing systems (ICDCS)*. IEEE, 183–195.
- [21] Serife Kucur Ergünay, Elie Khoury, Alexandros Lazaridis, and Sébastien Marcel. 2015. On the vulnerability of speaker verification to realistic voice spoofing. In *2015 IEEE 7th international conference on biometrics theory, applications and systems (BTAS)*. IEEE, 1–6.
- [22] Huan Feng, Kassem Fawaz, and Kang G Shin. 2017. Continuous authentication for voice assistants. In *Proceedings of the 23rd Annual International Conference on Mobile Computing and Networking*. 343–355.
- [23] Rainhard Dieter Findling, Tahmid Quddus, and Stephan Sigg. 2019. Hide my gaze with EOG! towards closed-eye gaze gesture passwords that resist observation-attacks with electrooculography in smart glasses. In *Proceedings of the 17th international conference on advances in mobile computing & multimedia*. 107–116.

- [24] Eira Friström, Elias Lius, Niki Ulmanen, Paavo Hietala, Pauliina Kärkkäinen, Tommi Mäkinen, Stephan Sigg, and Rainhard Dieter Findling. 2019. Free-form gaze passwords from cameras embedded in smart glasses. In *Proceedings of the 17th International Conference on Advances in Mobile Computing & Multimedia*. 136–144.
- [25] Bhanuka Gamage. 2024. AI-Enabled Smart Glasses for People with Severe Vision Impairments. *ACM SIGACCESS Accessibility and Computing* 137 (2024), 1–1.
- [26] Yaroslav Ganin and Victor Lempitsky. 2015. Unsupervised domain adaptation by backpropagation. In *International conference on machine learning*. PMLR, 1180–1189.
- [27] Yang Gao, Yincheng Jin, Jagmohan Chauhan, Seokmin Choi, Jiyang Li, and Zhanpeng Jin. 2021. Voice in ear: Spoofing-resistant and passphrase-independent body sound authentication. *Proceedings of the ACM on Interactive, Mobile, Wearable and Ubiquitous Technologies* 5, 1 (2021), 1–25.
- [28] Kaiyi Guo, Tianyu Wu, Yang Gao, Qian Zhang, and Dong Wang. 2025. EchoTouch: Low-power Face-touching Behavior Recognition Using Active Acoustic Sensing on Glasses. *Proc. ACM Interact. Mob. Wearable Ubiquitous Technol.* 9, 2, Article 31 (June 2025), 33 pages. doi:10.1145/3729481
- [29] Kaiyi Guo, Qian Zhang, and Dong Wang. 2025. EchoBreath: Continuous Respiratory Behavior Recognition in the Wild via Acoustic Sensing on Smart Glasses. In *Proceedings of the 2025 CHI Conference on Human Factors in Computing Systems (CHI '25)*. Association for Computing Machinery, New York, NY, USA, Article 348, 21 pages. doi:10.1145/3706598.3714171
- [30] Jibo He, Jake Ellis, William Choi, and Pingfeng Wang. 2015. Driving While Reading Using Google Glass Versus Using a Smartphone: Which is More Distracting to Driving Performance?. In *Driving Assessment Conference*, Vol. 8. University of Iowa.
- [31] Kaiming He, Xiangyu Zhang, Shaoqing Ren, and Jian Sun. 2016. Deep residual learning for image recognition. In *Proceedings of the IEEE conference on computer vision and pattern recognition*. 770–778.
- [32] Chenpei Huang, Hui Zhong, Pavana Prakash, Dian Shi, Xu Yuan, and Miao Pan. 2025. Eve said yes: Airbone authentication for head-wearable smart voice assistant. *IEEE Transactions on Mobile Computing* (2025).
- [33] Masaya Inoue and Kazuya Murao. 2024. User Authentication Method for Smart Glasses using Gaze Information of Registered Known Images and AI-generated Unknown Images. In *Companion of the 2024 on ACM International Joint Conference on Pervasive and Ubiquitous Computing*. 525–530.
- [34] MD Rasel Islam, Doyoung Lee, Liza Suraiya Jahan, and Ian Oakley. 2018. Glasspass: Tapping gestures to unlock smart glasses. In *Proceedings of the 9th Augmented Human International Conference*. 1–8.
- [35] Kaito Isobe and Kazuya Murao. 2021. Person-identification method using active acoustic sensing applied to nose. In *Proceedings of the 2021 ACM International Symposium on Wearable Computers*. 138–140.
- [36] Koji Iwano, Taro Miyazaki, and Sadaoki Furui. 2005. Multimodal speaker verification using ear image features extracted by PCA and ICA. In *International Conference on Audio-and Video-Based Biometric Person Authentication*. Springer, 588–596.
- [37] Madhu R Kamble, Hardik B Sailor, Hemant A Patil, and Haizhou Li. 2020. Advances in anti-spoofing: from the perspective of ASVspoof challenges. *APSIPA Transactions on Signal and Information Processing* 9 (2020), e2.
- [38] Lawrence George Kersta. 1962. Voiceprint identification. *The Journal of the Acoustical Society of America* 34, 5, Supplement (1962), 725–725.
- [39] Smita Khade, Swati Ahirrao, Shraddha Phansalkar, Ketan Kotecha, Shilpa Gite, and Sudeep D Thepade. 2021. Iris liveness detection for biometric authentication: A systematic literature review and future directions. *Inventions* 6, 4 (2021), 65.
- [40] Azizuddin Khan and Gyan Prakash. 2017. Design and implementation of smart glass with voice detection capability to help visually impaired people. *International Journal of MC Square Scientific Research* 9, 3 (2017), 54–59.
- [41] Sunwook Kim, Maury A Nussbaum, and Joseph L Gabbard. 2016. Augmented reality “smart glasses” in the workplace: industry perspectives and challenges for worker safety and health. *IIE transactions on occupational ergonomics and human factors* 4, 4 (2016), 253–258.
- [42] Huining Li, Chenhan Xu, Aditya Singh Rathore, Zhengxiong Li, Hanbin Zhang, Chen Song, Kun Wang, Lu Su, Feng Lin, Kui Ren, et al. 2020. VocalPrint: Exploring a resilient and secure voice authentication via mmWave biometric interrogation. In *Proceedings of the 18th Conference on Embedded Networked Sensor Systems*. 312–325.
- [43] Jingjin Li, Chao Chen, Mostafa Rahimi Azghadi, Hossein Ghodosi, Lei Pan, and Jun Zhang. 2023. Security and privacy problems in voice assistant applications: A survey. *Computers & Security* 134 (2023), 103448.
- [44] Ke Li, Devansh Agarwal, Ruidong Zhang, Vipin Gunda, Tianjun Mo, Saif Mahmud, Boao Chen, François Guimbretière, and Cheng Zhang. 2024. SonicID: User Identification on Smart Glasses with Acoustic Sensing. *Proceedings of the ACM on Interactive, Mobile, Wearable and Ubiquitous Technologies* 8, 4 (2024), 1–27.
- [45] Yue Li, Xueru Gao, Qipeng Song, Yao Wang, Pin Lyu, and Haibin Zhang. 2024. BoneAuth: A Bone Conduction-Based Voice Liveness Authentication for Voice Assistants. *IEEE Internet of Things Journal* (2024).
- [46] Yung-Hui Li and Po-Jen Huang. 2017. An accurate and efficient user authentication mechanism on smart glasses based on iris recognition. *Mobile Information Systems* 2017, 1 (2017), 1281020.
- [47] Zhuohang Li, Cong Shi, Tianfang Zhang, Yi Xie, Jian Liu, Bo Yuan, and Yingying Chen. 2021. Robust Detection of Machine-induced Audio Attacks in Intelligent Audio Systems with Microphone Array. In *Proceedings of the 2021 ACM SIGSAC Conference on Computer and Communications Security (Virtual Event, Republic of Korea) (CCS '21)*. Association for Computing Machinery, New York, NY, USA, 1884–1899. doi:10.1145/3460120.3484755
- [48] Hyunchul Lim, Guilin Hu, Richard Jin, Hao Chen, Ryan Mao, Ruidong Zhang, and Cheng Zhang. 2023. C-Auth: Exploring the Feasibility of Using Egocentric View of Face Contour for User Authentication on Glasses. In *Proceedings of the 2023 ACM International Symposium on Wearable Computers*. 6–10.

- [49] Rui Liu, Cory Cornelius, Reza Rawassizadeh, Ronald Peterson, and David Kotz. 2018. Vocal Resonance: Using Internal Body Voice for Wearable Authentication. *Proc. ACM Interact. Mob. Wearable Ubiquitous Technol.* 2, 1, Article 19 (March 2018), 23 pages. doi:10.1145/3191751
- [50] Isaias Majil, Mau-Tsuen Yang, and Sophia Yang. 2022. Augmented reality based interactive cooking guide. *Sensors* 22, 21 (2022), 8290.
- [51] Amit Meghanani, Chandran Savithri Anoop, and AG Ramakrishnan. 2021. An exploration of log-mel spectrogram and MFCC features for Alzheimer’s dementia recognition from spontaneous speech. In *2021 IEEE spoken language technology workshop (SLT)*. IEEE, 670–677.
- [52] Yan Meng, Jiachun Li, Matthew Pillari, Arjun Deopujari, Liam Brennan, Hafsa Shamsie, Haojin Zhu, and Yuan Tian. 2022. Your microphone array retains your identity: A robust voice liveness detection system for smart speakers. In *31st USENIX Security Symposium (USENIX Security 22)*. 1077–1094.
- [53] Johannes Meyer, Adrian Frank, Thomas Schlebusch, and Enkelejda Kasneci. 2022. U-har: A convolutional approach to human activity recognition combining head and eye movements for context-aware smart glasses. *Proceedings of the ACM on Human-Computer Interaction* 6, ETRA (2022), 1–19.
- [54] Minh Tuan Nguyen, Wei Wen Lin, and Jin H Huang. 2023. Heart sound classification using deep learning techniques based on log-mel spectrogram. *Circuits, Systems, and Signal Processing* 42, 1 (2023), 344–360.
- [55] AN Nithyaa, R Premkumar, N Sudhandirapriya, and R Durga. 2023. Eye Glasses for the Visually Challenged Using Artificial Intelligence Application. In *International Conference on Soft Computing and Signal Processing*. Springer, 347–360.
- [56] Francesca Palermo, Luca Casciano, Lokmane Demagh, Aurelio Teliti, Niccolò Antonello, Giacomo Gervasoni, Hazem Hesham Yousef Shalby, Marco Brando Paracchini, Simone Mentasti, Hao Quan, et al. 2025. Advancements in Context Recognition for Edge Devices and Smart Eyewear: Sensors and Applications. *IEEE Access* (2025).
- [57] Ge Peng, Gang Zhou, David T Nguyen, Xin Qi, Qing Yang, and Shuangquan Wang. 2016. Continuous authentication with touch behavioral biometrics and voice on wearable glasses. *IEEE transactions on human-machine systems* 47, 3 (2016), 404–416.
- [58] Yue Qin, Chun Yu, Zhaoheng Li, Mingyuan Zhong, Yukang Yan, and Yuanchun Shi. 2021. Proximic: Convenient voice activation via close-to-mic speech detected by a single microphone. In *Proceedings of the 2021 CHI Conference on Human Factors in Computing Systems*. 1–12.
- [59] Xinghua Qu, Pengfei Wei, Mingyong Gao, Zhu Sun, Yew Soon Ong, and Zejun Ma. 2022. Synthesising audio adversarial examples for automatic speech recognition. In *Proceedings of the 28th ACM SIGKDD Conference on Knowledge Discovery and Data Mining*. 1430–1440.
- [60] P. Selvi Rajendran, Padmaveni Krishnan, and D. John Aravindhar. 2020. Design and Implementation of Voice Assisted Smart Glasses for Visually Impaired People Using Google Vision API. In *2020 4th International Conference on Electronics, Communication and Aerospace Technology (ICECA)*. 1221–1224. doi:10.1109/ICECA49313.2020.9297553
- [61] P Selvi Rajendran, Padmaveni Krishnan, and D John Aravindhar. 2020. Design and implementation of voice assisted smart glasses for visually impaired people using google vision api. In *2020 4th International Conference on Electronics, Communication and Aerospace Technology (ICECA)*. IEEE, 1221–1224.
- [62] Md Sahidullah, Dennis Alexander Lehmann Thomsen, Rosa Gonzalez Hautamäki, Tomi Kinnunen, Zheng-Hua Tan, Robert Parts, and Martti Pitkänen. 2017. Robust voice liveness detection and speaker verification using throat microphones. *IEEE/ACM Transactions on Audio, Speech, and Language Processing* 26, 1 (2017), 44–56.
- [63] Stefan Schneegass, Youssef Oualil, and Andreas Bulling. 2016. SkullConduct: Biometric user identification on eyewear computers using bone conduction through the skull. In *Proceedings of the 2016 CHI Conference on Human Factors in Computing Systems*. 1379–1384.
- [64] Hyejin Shin, Jun Ho Huh, Bum Jun Kwon, Iljoo Kim, Eunyong Cheon, HongMin Kim, Choong-Hoon Lee, and Ian Oakley. 2024. SkullID: Through-skull sound conduction based authentication for smartglasses. In *Proceedings of the 2024 CHI Conference on Human Factors in Computing Systems*. 1–19.
- [65] Sayaka Shiota, Fernando Villavicencio, Junichi Yamagishi, Nobutaka Ono, Isao Echizen, and Tomoko Matsui. 2015. Voice liveness detection algorithms based on pop noise caused by human breath for automatic speaker verification. In *INTERSPEECH 2015 16th Annual Conference of the International Speech Communication Association*. International Speech Communication Association, France, 239–243.
- [66] Tao Sun, Yankai Zhao, Wentao Xie, Jiao Li, Yongyu Ma, and Jin Zhang. 2024. EyeGesener: Eye gesture listener for smart glasses interaction using acoustic sensing. *Proceedings of the ACM on Interactive, Mobile, Wearable and Ubiquitous Technologies* 8, 3 (2024), 1–28.
- [67] Ashique T P, Hridya Girish, Ivine P Sabu, Thomas Raju, and Anoop V. 2025. AI-Powered Smart Glasses for Real-Time Speech-to-Text Transcription. In *2025 4th International Conference on Advances in Computing, Communication, Embedded and Secure Systems (ACCESS)*. 442–445. doi:10.1109/ACCESS65134.2025.11135871
- [68] Eric Tzeng, Judy Hoffman, Kate Saenko, and Trevor Darrell. 2017. Adversarial discriminative domain adaptation. In *Proceedings of the IEEE conference on computer vision and pattern recognition*. 7167–7176.
- [69] Suresh Veesa and Madhusudan Singh. 2025. Deep learning countermeasures for detecting replay speech attacks: a review. *International Journal of Speech Technology* 28, 1 (2025), 39–51.
- [70] Qian Wang, Xiu Lin, Man Zhou, Yanjiao Chen, Cong Wang, Qi Li, and Xiangyang Luo. 2019. VoicePop: A Pop Noise based Anti-spoofing System for Voice Authentication on Smartphones. In *IEEE INFOCOM 2019 - IEEE Conference on Computer Communications*. 2062–2070. doi:10.1109/INFOCOM.2019.8737422
- [71] Yao Wang, Wandong Cai, Tao Gu, Wei Shao, Yannan Li, and Yong Yu. 2019. Secure your voice: An oral airflow-based continuous liveness detection for voice assistants. *Proceedings of the ACM on interactive, mobile, wearable and ubiquitous technologies* 3, 4 (2019), 1–28.
- [72] Zeyu Wang, Yuanchun Shi, Yuntao Wang, Yuchen Yao, Kun Yan, Yuhan Wang, Lei Ji, Xuhai Xu, and Chun Yu. 2024. G-VOILA: gaze-facilitated information querying in daily scenarios. *Proceedings of the ACM on Interactive, Mobile, Wearable and Ubiquitous Technologies* 8, 2 (2024), 1–33.

- [73] Emily Wenger, Max Bronckers, Christian Cianfarani, Jenna Cryan, Angela Sha, Haitao Zheng, and Ben Y Zhao. 2021. "Hello, It's Me": Deep Learning-based Speech Synthesis Attacks in the Real World. In *Proceedings of the 2021 ACM SIGSAC Conference on Computer and Communications Security*. 235–251.
- [74] Christian Winkler, Jan Gugenheimer, Alexander De Luca, Gabriel Haas, Philipp Speidel, David Dobbstein, and Enrico Rukzio. 2015. Glass unlock: Enhancing security of smartphone unlocking through leveraging a private near-eye display. In *Proceedings of the 33rd annual acm conference on human factors in computing systems*. 1407–1410.
- [75] Chen Yan, Xiaoyu Ji, Kai Wang, Qinhong Jiang, Zizhi Jin, and Wenyuan Xu. 2022. A survey on voice assistant security: Attacks and countermeasures. *Comput. Surveys* 55, 4 (2022), 1–36.
- [76] Chen Yan, Yan Long, Xiaoyu Ji, and Wenyuan Xu. 2019. The catcher in the field: A fieldprint based spoofing detection for text-independent speaker verification. In *Proceedings of the 2019 ACM SIGSAC Conference on Computer and Communications Security*. 1215–1229.
- [77] Jiangyan Yi, Chenglong Wang, Jianhua Tao, Xiaohui Zhang, Chu Yuan Zhang, and Yan Zhao. 2023. Audio deepfake detection: A survey. *arXiv preprint arXiv:2308.14970* (2023).
- [78] Linghan Zhang, Sheng Tan, Yingying Chen, and Jie Yang. 2022. A Continuous Articulatory-Gesture-Based Liveness Detection for Voice Authentication on Smart Devices. *IEEE Internet of Things Journal* 9, 23 (2022), 23320–23331. doi:10.1109/JIOT.2022.3199995
- [79] Linghan Zhang, Sheng Tan, and Jie Yang. 2017. Hearing your voice is not enough: An articulatory gesture based liveness detection for voice authentication. In *Proceedings of the 2017 ACM SIGSAC Conference on Computer and Communications Security*. 57–71.
- [80] Linghan Zhang, Sheng Tan, Jie Yang, and Yingying Chen. 2016. Voicelive: A phoneme localization based liveness detection for voice authentication on smartphones. In *Proceedings of the 2016 ACM SIGSAC Conference on Computer and Communications Security*. 1080–1091.
- [81] Rui Zhang, Zheng Yan, Xuerui Wang, and Robert H Deng. 2022. Livoauth: Liveness detection in voiceprint authentication with random challenges and detection modes. *IEEE Transactions on Industrial Informatics* 19, 6 (2022), 7676–7688.
- [82] Tianfang Zhang, Qiufan Ji, Zhengkun Ye, Md Mojibur Rahman Redoy Akanda, Ahmed Tanvir Mahdad, Cong Shi, Yan Wang, Nitesh Saxena, and Yingying Chen. 2024. SAFARI: Speech-Associated Facial Authentication for AR/VR Settings via Robust Vibration Signatures. In *Proceedings of the 2024 ACM SIGSAC Conference on Computer and Communications Security*. 153–167.
- [83] Yongtuo Zhang, Wen Hu, Weitao Xu, Chun Tung Chou, and Jiankun Hu. 2018. Continuous authentication using eye movement response of implicit visual stimuli. *proceedings of the acm on interactive, mobile, wearable and ubiquitous technologies* 1, 4 (2018), 1–22.
- [84] Zhan Zhang, Enze Bai, Aram Stepanian, Swathi Jagannath, and Sun Young Park. 2025. Touchless interaction for smart glasses in emergency medical services: user needs and experiences. *International Journal of Human-Computer Interaction* 41, 5 (2025), 2984–3003.
- [85] Chu-Xiao Zuo, Zhi-Jun Jia, and Wu-Jun Li. 2024. AdvTTS: Adversarial Text-to-Speech Synthesis Attack on Speaker Identification Systems. In *ICASSP 2024-2024 IEEE International Conference on Acoustics, Speech and Signal Processing (ICASSP)*. IEEE, 4840–4844.

Received 20 February 2007; revised 12 March 2009; accepted 5 June 2009